COBEM 2023 27TH INTERNATIONAL CONGRESS OF MECHANICAL ENGENEERING

ABCM Brazilian Society of Mechanical Sciences and Engineering
27th ABCM International Congress of Mechanical Engineering
December 04-08, 2023, Florianópolis-SC, Brazil

COB-2023-0612
A PARAMETRIC INVESTIGATION OF LOW VELOCITY IMPACT IN SMA-COMPOSITE PLATES

Lucas L. Vignoli
Center of Technology and Applications of Composite Materials, Department of Mechanical Engineering, Federal University of Rio de Janeiro, Macaé, RJ, Brazil
ll.vignoli@mecanica.coppe.ufrj.br

Arthur Adeodato
State University of do Rio de Janeiro – UERJ/IPRJ, Nova Friburgo, RJ, Brazil
arthuradeodato@iprj.uerj.br

Abstract. *Structures made by composite materials have been very explored for many industries, like aeronautic, automotive and marine. Composite materials have lightweight and high stiffness and strength characteristic; however, the low impact resistance of these materials is a major drawback. This is primarily because composite structures have a limited capability to withstand transversal loads. Especially low velocity impacts are very dangerous because they may induce imperceptible damages on routine inspections. For instance, the literature indicates that around 15% of repairs performed in airplanes are results from low velocity impacts, like dropping a tool on a part of the airplane's structure. Alternatively, shape memory alloys (SMAs) have been proposed as a potential solution to this issue due to their ability to dissipate energy through pseudoelasticity. Hence, exploring the combination of SMA plies in composite laminates seems to be a promising way to avoid impact issues. The goal of the present investigation is to carry out a parametric study of impacts in composite plates with and without SMA reinforced. Three parameters are evaluated: the fiber volume fraction, the SMA ply thickness and the SMA arrangement in the laminate. The simulations are carried out using the commercial finite element software Ansys. The Puck failure criterion is considered for the laminate and Auricchio's constitutive model is applied for the SMA. The results show that using a thin SMA ply can significantly improve the impact resistance of laminates, reducing and even eliminating structural damage from low velocity impacts. These findings have implications for the design concerning cost and weight-efficient structures.*

Keywords: *SMA, SMA hybrid composite, low velocity impact, damage*

1. INTRODUCTION

Structures made from composite materials have been extensively investigated and used in the different industries. This fact can be attributed to the excellent characteristics inherent to this type of material, such as corrosion resistance, high stiffness and strength, low specific weight and fatigue resistance (Herakovich, 2012).

For design composite structures, many variables are involved because the multiphase and multiscale characteristics (Tsai & Melo, 2014). To deal with this issue, micromechanical models are efficient tools (Ha et al., 2008; Vignoli et al., 2019; Lin, 2022). To improve the analysis efficiency, analytical micromechanical modeling strategies have been proposed and demonstrated to have good performance when compared with experimental and numerical results (Andrianov et al., 2018; Vignoli et al., 2021). However, for macromechanical analysis, the numerical simulation seems indispensable (Shah, 2010). This hybrid analytical-numerical approach was performed for different structures, like pressure vessels (Vignoli & Savi, 2018) and notched plates (Vignoli et al., 2020a; Vignoli et al., 2022a). A numerical multiscale analysis for impact problems was proposed by Staniszewski et al. (2022); however, the computational cost becomes an issue for parametric studies.

One of the biggest concerns and reasons for reduced reliability when it comes to composite materials is their low impact strength. According to Andrew et al. (2019), almost 13% of repairs performed on Boeing 747 aircraft are due to impacts from external objects. In collaboration with this, Topac et al. (2017) explain that low velocity transverse impacts, such as dropping a tool on a part of the airplane's structure, generate internal damage that is not visible in routine inspections. The impact problem in composites for pipes and wind turbines are also reported by Shahveisi & Feli (2022) and Pinto et al. (2021), respectively.

Therefore, many engineering procedures already consider that the composite parts have these damages in the planning phase, something that ends up adding weight to the structure. The importance of tools for damage monitoring is highlighted by Arumugam et al. (2015), Thiene & Galvanetto (2015) and Talreja & Phan (2019). An additional difficult becomes from the fact that many different damage mechanisms may happen (Tita et al., 2008).

To improve the impact resistance in composite structures, the hybridization approach has been proposed. For instance, Güneş & Şahin (2020) propose to use carbon and glass fiber in the same laminate. The impact performance of glass fiber reinforced plastic (GFRP) can be improved adding metallic layers. However, traditional metals allow undesirable residual stresses and strains (Starikov, 2013; Chai & Manikandan, 2014). An alternative to avoid residual stresses and strains is the use of shape memory alloy (SMA), which is very useful for dynamical loads to explore the pseudoelastic effect (Savi, 2015; Vignoli et al., 2020b). Pseudoelasticity is the phenomenon resultant from micromechanical austenite-martensite phase transformation in SMAs, generating a hysteresis looping and dissipating energy (Paiva & Savi, 2006; Lagoudas, 2008).

Zhao et al. (2018) and Gupta et al. (2019) presented experimental studies indicating that SMA may improve the impact response of GFRP. Lester et al. (2015) reviewed and proposed many advantages and application for composites with SMA. One of the most considerable perspectives is related to improve the composite performance when submitted to impact (Debossan & Vignoli, 2022).

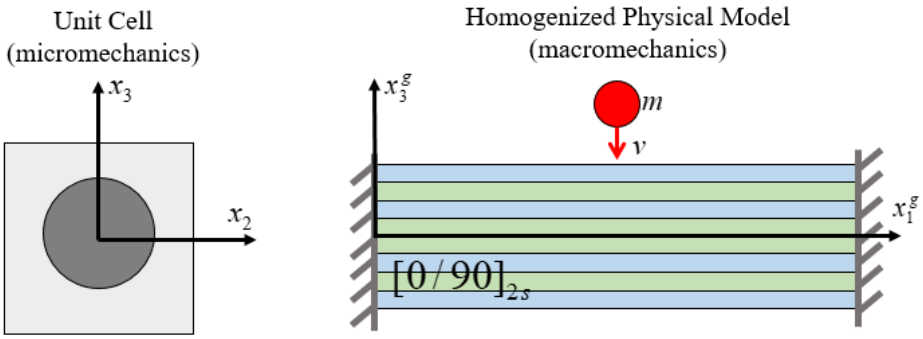

Figure 1: Schematic representation of the proposed multiscale procedure.

Considering these points, the present work aims to perform an analytical-numerical multiscale analysis of hybrid GFRP laminates reinforced with SMA. Figure 1 shows the main idea of the proposed methodology described in Section 2. Considering that fiber volume fraction influences on the laminate impact response (Melo & Villena, 2012), the VSPKc micromechanical model is described in Section 2.1 to evaluate the GFRP lamina properties from glass fiber and epoxy matrix properties. A cross-ply laminate $[0/90]_{2s}$ is considered for macromechanical analysis using the commercial finite element software Ansys. For a detailed discussion about stacking sequence effects, see Hongkarnjanakul et al., (2013) and Wang et al. (2021). The effective properties obtained in Section 2.1 are used as input to the homogenized ply model described in Section 2.2. Note that the laminate properties are defined based on the material coordinate system for each lamina, x_i, where $x_1 \equiv x_1^g$ for laminae oriented at 0 and $x_1 \equiv x_2^g$ for laminae oriented at 90. The laminated is submitted to a perpendicular low velocity impact. The impactor is assumed as cylindrical with the longitudinal axis parallel to x_2^g. An investigation about different impactor shape can be found in Kursun et al. (2016). SMA reinforced are evaluated when applied on the two top plies oriented at 0. The results are presented and discussed in Section 3 and the main conclusions are summarized in Section 4.

2. MULTISCALE MODELING

Multiscale modeling first considers a micromechanical level, assessing how fiber and matrix properties influence lamina's effective properties according to the constituents' volume fraction. Subsequently, a macromechanical study is carried out that evaluates the macroscopic behavior of the laminate when it is subjected to a low velocity impact, also allowing the use of proper failure criteria to assess damage in the composite material.

2.1 Analytical Micromechanical Model

The first step of multiscale modeling is the use of VSPKc micromechanical model proposed by Vignoli et al. (2022b) to estimate the following effective elastic properties of the lamina: longitudinal elastic, E_1; in-plane Poisson's ratio, ν_{12}; transversal elastic modulus, E_2; in-plane shear modulus, G_{12}; and out-of-plane shear modulus, G_{23}.

For E_1 and ν_{12}, the equations are similar to the classical estimation of the rule of mixture. Alternatively, for E_2, G_{12} and G_{23} the model is able to consider fiber circular cross section and a square symmetry of the unit cell. The following set of equations is stablished to estimate the elastic properties based on VSPKc model:

$$E_1 = E_1^f V_f + E^m(1-V_f) \tag{1}$$

$$\nu_{12} = \nu_{12}^f V_f + \nu^m(1-V_f) \tag{2}$$

$$E_2 = E^m\left\{1+2\sqrt{\frac{V_f}{\pi}}\left[\frac{\pi}{2a_{22}} - \frac{\ln\left(a_{22}+\sqrt{{a_{22}}^2-1}\right)}{a_{22}\sqrt{{a_{22}}^2-1}} - 1\right]\right\} \tag{3}$$

$$G_{12} = G^m\left\{1+2\sqrt{\frac{V_f}{\pi}}\left[\frac{\pi}{2a_{12}} - \frac{\ln\left(a_{12}+\sqrt{{a_{12}}^2-1}\right)}{a_{12}\sqrt{{a_{12}}^2-1}} - 1\right]\right\} \tag{4}$$

$$G_{23} = G^m\left\{1+2\sqrt{\frac{V_f}{\pi}}\left[\frac{\pi}{2a_{23}} - \frac{\ln\left(a_{23}+\sqrt{{a_{23}}^2-1}\right)}{a_{23}\sqrt{{a_{23}}^2-1}} - 1\right]\right\} \tag{5}$$

where E_1^f is the fiber longitudinal elastic modulus, E_2^f is the fiber transversal elastic modulus, ν_{12}^f is the fiber in-plane Poisson's ratio, G_{12}^f is the fiber in-plane shear modulus, G_{23}^f is the fiber out-of-plane shear modulus, E^m is the matrix elastic modulus, ν^m is the matrix Poisson's ratio, $G^m = E^m/2(1+\nu^m)$ is the matrix shear modulus and V_f is the fiber volume fraction. Additionally, $a_{22} = 2[(E^m/E_2^f)-1]\sqrt{V_f/\pi}$, $a_{12} = 2[(G^m/G_{12}^f)-1]\sqrt{V_f/\pi}$ and $a_{23} = 2[(G^m/G_{23}^f)-1]\sqrt{V_f/\pi}$.

To evaluate the damage, it is necessary to calculate lamina longitudinal tensile strength, S_{11}^t, longitudinal compressive strength, S_{11}^c, transversal tensile strength, S_{22}^t, transversal compressive strength, S_{22}^c, in-plane shear strength, S_{12}^s, and out-of-plane shear strength, S_{23}^s.

According to Vignoli et al. (2020c), S_{11}^t and S_{11}^c can be estimated considering that fiber tensile and compressive strength, S_t^f and S_c^f, respectively, have an average reduction of 8% for tension and 20% for compression. For tension, the strength reduction is related to in situ damage during manufacturing; for compression, fiber misalignment induces additional bending to the compressive load. Additionally, for S_{12}^s the authors proposed a closed-form relation based on the concentric cylinder model.

For transversal strengths, Vignoli et al. (2020d) proposed that S_{22}^t is governed by matrix dilatation energy density, S_{22}^c is defined based on the fiber-matrix interface and S_{23}^s tends to be close to the matrix shear strength, S_s^m.

Based in this assumptions, lamina strengths are computed by

$$S_{11}^t = \left[V_f + (1-V_f)\left(\frac{E^m}{E_1^f}\right)\right]0.92S_t^f \tag{6}$$

$$S_{11}^c = \left[V_f + (1-V_f)\left(\frac{E^m}{E_1^f}\right)\right]0.8S_c^f \tag{7}$$

$$S_{22}^t = \frac{1}{(1+\nu^m)(1-2\beta)g_t}\sqrt{\left(\frac{6E^m}{1+2\nu^m}\right)u_v^c} \tag{8}$$

$$S_{22}^c = \frac{S^i}{\sqrt{g_{ic}}}\left(\frac{2}{1-\beta}\right) \tag{9}$$

$$S_{12}^s = \frac{S_s^m}{2}\left[\frac{(G_{12}^f+G^m)+(G_{12}^f-G^m)V_f}{G_{12}^f}\right] \tag{10}$$

$$S_{23}^s = S_s^m \tag{11}$$

where u_v^c is the matrix critical dilatation energy density, S^i is the interface strength, $\alpha = (G^m \kappa^f - G_{23}^f \kappa^m)/(G_{23}^f + G^m \kappa^f)$, $\beta = (G^m - G_{23}^f)/(G^m + G_{23}^f \kappa^m)$, $\gamma = (\alpha - \beta)/[(1-\beta) - \beta(1-\alpha)]$, $\kappa^m = 3 - 4\nu^m$, $\kappa^f = 3 - 4\nu_{23}^f$, $g_t = g_t(V_f) = 1 - 5.8\gamma V_f^{\,3}$ and $g_{ic} = g_{ic}(V_f) = -7.71(0.14+\beta)V_f^{\,3} + 6.63(0.01+\beta)V_f^{\,2} + +0.16(3+\beta)V_f - 0.76(-0.24+\beta)$.

2.2 Numerical Macromechanical Model

Due to the symmetry of the problem, only half of the laminate geometry is considered, as shown in Fig. 2a. The boundary conditions represent that perpendicular displacements are zero for the following cases: on the half symmetry plane, where just vertical displacement is allowed; on the faces perpendicular to x_2^g, due to the periodicity condition assumed. A mesh example around the impact region is presented in Fig. 2b, where quadratic SOLID186 element is used.

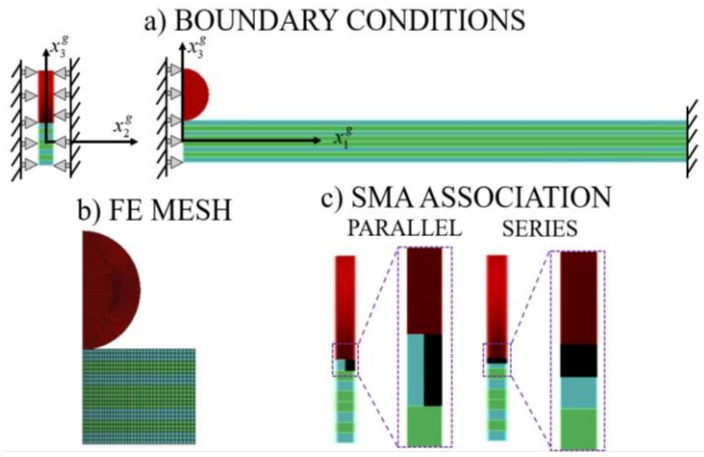

Figure 2: Summary of the FE model: a) boundary conditions; b) example of the FE mesh; c) SMA association in parallel and in series at the laminate top plies (SMA in black).

The contacts between plies are defined as bonded, not allowing slippage and neither separation between the laminae. The contact in the impact region is defined as Frictional, with coefficient of friction equal to 0.3 (Liu et al., 2016; Wang et al., 2020). Additionally, cohesive model elements are required in ply-to-ply contacts (Kubair & Lakshmana, 2008). Considering mode II delamination assuming maximum equivalent contact stress equal to matrix shear strength, 50MPa (Kaddour & Hinton, 2012), and critical fracture energy for tangential slip equal to 0.208mJ/mm^2 (Oliveira & Donadon, 2020).

Three different set of simulations are performed: i) with all plies made by GFRP; ii) including a SMA in parallel at the first two plies, both oriented at 0; iii) including SMA is series also with first two plies, keeping the total thickness of the laminate constant. The difference between SMA association in parallel and in series is presented in Fig. 2c. For the second and the third one, the influence of SMA volume fraction on the top ply is analyzed for V_f = 0 .1, 0.3 and 0.5. Additionally, the fiber volume fractions V_f = 0.3, 0.5 and 0.7 are evaluated. Hence, a total of 21 simulations is carried out, combining fiber and SMA volume fractions, as well as different possibilities of SMA associations.

The goal of studying the application of SMA is to explore the pseudoelastic phenomenon, resulted from the SMA phase transformation. As illustrated in Fig. 3, SMA initially has austenitic microstructure and presents a linear behavior when subjected to mechanical loading up to σ_s^{AM}. Increasing the load, a phase transformation from austenite to martensite occurs and total transformation is achieved in σ_f^{AM}, followed by a linear response. For unloading, an initial linear behavior is observed and reverse transformation starts in σ_s^{MA} and finishes in σ_s^{MA}. E_A and E_M are the elastic moduli of austenite and martensite phases, respectively, and ε_R is the maximum recoverably strain. Due to the different paths taken in stress-strain curves for load and unload, hysteresis loop is generated and dissipates energy. The constitutive model proposed by Auricchio et al. (1997) is used for the SMA in the present study.

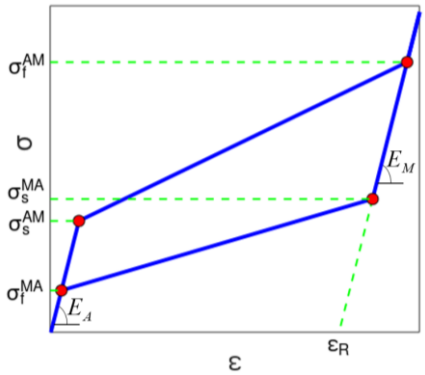

Figura 3: Typical pseudoelastic behavior for SMA.

To properly evaluate the damage on the composite, the Puck failure criterion (Puck & Schurmann, 1998) is applied considering the World-Wide Failure Exercise (WWFE) recommendations (Hinton et al., 2004). Puck criterion is able to evaluate four different damage modes: fiber in tension, fiber in compression, matrix in tension and matrix in compression. For damage propagation, the following material properties degradation are adopted: 0.93 for fiber in tension, 0.86 for fiber in compression, 0.80 for matrix in tension and 0.6 for matrix in compression (Vignoli & Castro, 2021).

3. RESULTS

The studied plate has a ply-thickness of 0.5 mm, reaching a total thickness of 8 mm, and a length of 200 mm. The constituents' properties required as input for the VSPKc micromechanical model are presented in Table 1. The composite is made by glass fibers and epoxy matrix. Note that $G_{12}^f = G_{23}^f = E_1^f / 2(1+\nu_{12}^f)$ since glass fiber is isotropic. The properties of the SMA are listed in Table 2. Considering the drop of a metallic tool from a height of 1.50m, an impactor initial velocity of 5.29m/s is assumed.

Table 1: Constituents' properties for the micromechanical model (Kaddour & Hinton, 2012; Vignoli *et al.*, 2020d).

$E_1^f = E_2^f$	ν_{12}^f	E^m	ν^m
74GPa	0.2	4.08GPa	0.38
S_t^f	S_c^f	S_s^m	S_c^m
2150MPa	1450MPa	50MPa	120MPa
	u_v^c	S^i	
	0.18MPa	52MPa	

Table 2: SMA material properties (Alves *et al.*, 2018; Enemark *et al.*, 2014)

E_A	E_M	ν	σ_s^{AM}	σ_f^{AM}	σ_s^{MA}	σ_f^{MA}	ε_R
44.5GPa	25.8GPa	0.3	156.3MPa	373.0MPa	186.3MPa	61.6MPa	4.08%

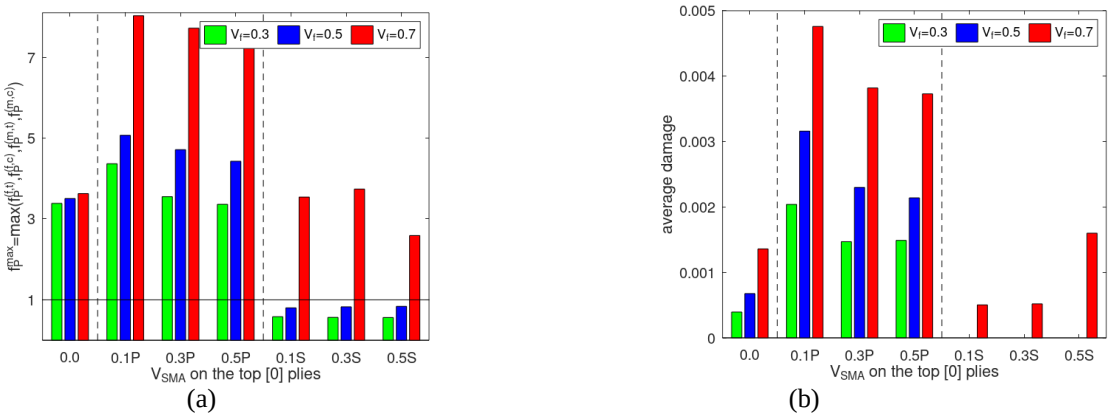

(a) (b)

Figure 4: Results of the parametric analysis for damage evaluation: a) maximum Puck failure function; b) Average damage in the laminate.

Puck failure function, $f_P^{\max}$, for the simulated laminates are presented in Fig. 4a, where $f_P^{(f,t)}$ is the fiber tensile failure function, $f_P^{(f,c)}$ is the fiber compressive failure function, $f_P^{(m,t)}$ is the matrix tensile failure function and $f_P^{(m,c)}$ is the matrix compressive failure function. Damage is present when $f_P^{\max} \geq 1$. The average damage is presented in Fig. 4b, where 0 means absence of damage and 1 means the whole volume of the laminate damaged.

The results indicate damage for: the laminates without SMA reinforcement; all the cases of SMA association in parallel, represented by the letter P; and for $V_f = 0.7$ when SMA is attached in series with top composite layers, represented by the letter S. There is no damage detected when SMA is in series for laminates with $V_f = 0.3$ and $V_f = 0.5$ .An increase of average damage is detected for the cases of SMA in parallel and a decrease in, even elimination in some cases, for the cases of SMA in series. There is not any fiber damage neither delamination for all these simulations; just matrix damage. Since just matrix damage is observed, damage is increasing according to the fiber volume fraction because the lamina transversal strengths decreases when V_f increases.

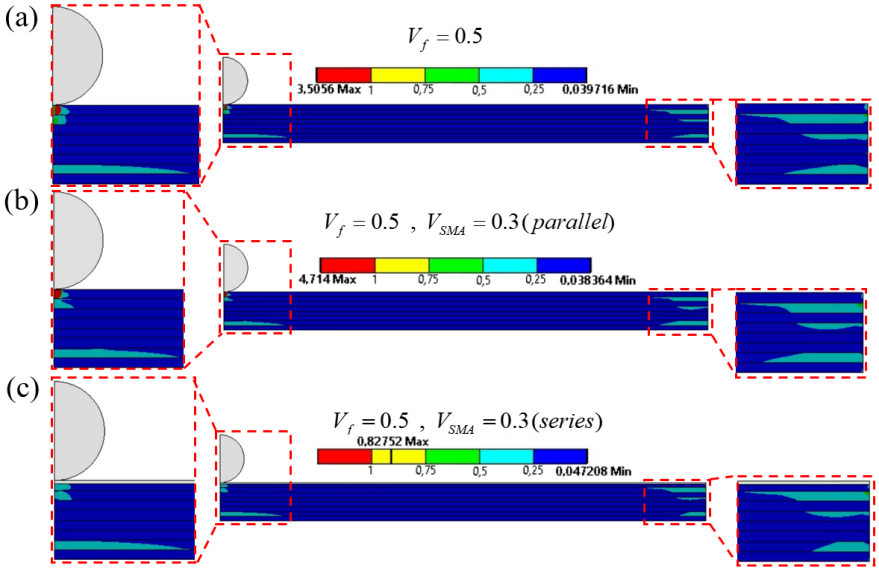

Figure 5: Puck failure criterion functions for $V_f = 0.5$: a) without SMA reinforce; b) SMA in parallel with $V_{SMA} = 0.3$; b) SMA in series with $V_{SMA} = 0.3$.

For a detailed analysis, the laminate with $V_f = 0.5$ is evaluated for the structures without SMA and with $V_{SMA} = 0.3$ associated in parallel and in series. Figure 5 shows the maximum Puck failure functions observed during the simulation for each case. The critical region is on the top layers around the contact impact. The failure function distribution on the fixed side (right) is very similar for the three cases. This very localized damage is a characteristic of low velocity impacts.

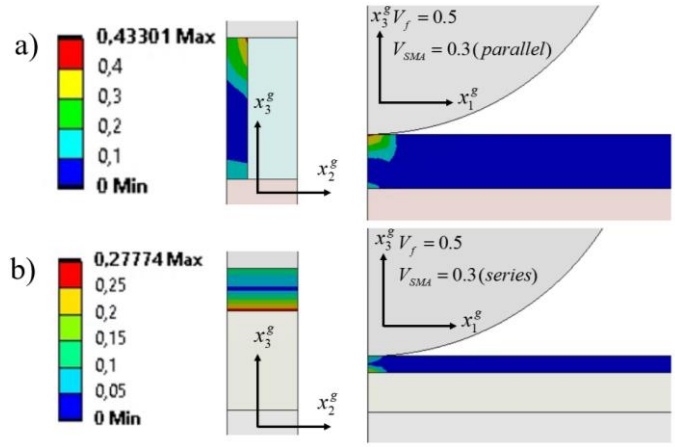

Figure 6: Maximum martensite volume fraction for $V_f = 0.5$ and $V_{SMA} = 0.3$: a) SMA in parallel; b) SMA in series.

To understand why SMA in series obtained the best results, Fig. 6 shows the martensite volume fraction distribution also for $V_f = 0.5$ and $V_{SMA} = 0.3$ on the top layers. Despite there is a higher phase transformation for SMA in parallel than in series, the phase transformation has a very irregular distribution for the first one, while a uniform distribution is realized for the second one. In fact, association in series with the applied boundary conditions (see Fig. 2a) is similar to the plane strain assumption, where the results must be independent of x_2^g. Additionally, when austenite-martensite phase transformation occurs, i.e. the pseudoelastic phenomenon, there is a decreasing of SMA stiffness and energy is dissipated. For SMA in parallel, when there is a stiffness reduction in this reinforce, the top glass fiber plies absorb a higher amount of load to obey the kinematical compatibility. On the other hand, an amount of energy is dissipated by the SMA phase transformation and a smaller strain deformation energy is stored on the glass fiber laminae for series association.

4. CONCLUSION

The present investigation evaluates different strategies to improve GFRP impact performance using SMA. A multiscale analysis is carried out using VSPKc micromechanical analytical model and finite element simulations using the software Ansys. The influence of fiber volume fraction is evaluated, as well as the SMA volume fraction on the top layers and its association. Damage reduction is observed in the presence of the SMA material. The reason for that fact is due to the hysteresis associated with the martensite phase transformation, which dissipates energy from the impact. The results indicate that add SMA in series is the best approach and even a small amount of SMA may decrease or eliminate the damage from impact load.

5. ACKNOWLEDGEMENTS

The authors would like to acknowledge the support of the Brazilian Research Agency FAPERJ.

6. REFERENCES

Alves, M.T.S., Steffen Jr., V., Santos, M.C., Savi, M.A., Enemark, S., Santos, I.F., 2018, “Vibration control of a flexible rotor suspended by shape memory alloy wires”, Journal of Intelligent Material Systems and Structures, 29, 2309–2323.

Andrew, J.J., Srinivasan, S.M., Arockiarajan, A., Dhakal, H.N., 2019, “Parameters influencing the impact response of fiber-reinforced polymer matrix composite materials: A critical review”, Composite Structures, 224, 111007.

Andrianov IV, Awrejcewicz J, Danishevs’kyy VV. Asymptotical Mechanics of Composites – Modelling Composites without FEM, Springer, 2018.

Arumugam, V., Sidharth, A.P., Santulli, C., 2015, “Characterization of failure modes in compression-after impact of glass–epoxy composite laminates using acoustic emission monitoring”, J Braz. Soc. Mech. Sci. Eng., 37, 1445–1455.

Auricchio, F., Taylor, R.L., Lubliner, J., 1997, “Shape-memory alloys: macromodeling and numerical simulations of the superelastic behavior”, Computational Methods in Applied Mechanical Engineering, 146, 281–312.

Chai, G.B., Manikandan, P., 2014, “Low velocity impact response of fibre-metal laminates – A review”, Composite Structures, 107, 363–381.

Debossan, A.J.D., Vignoli, L.L., 2022, “Improving Composite Low Velocity Impact Performance Using SMA: A Multiscale Analysis”, Mechanics Research Communications, 125, 103996.

Enemark, S., Savi, M.A., Santos, I.F., 2014, “Nonlinear dynamics of a pseudoelastic shape memory alloy system: theory and experiment”, Smart Materials and Structures, 23, 085018.

Güneş, A., Şahin, O.S., 2020, “Investigation of the effect of surface crack on low-velocity impact response in hybrid laminated composite plates”, Journal of the Brazilian Society of Mechanical Sciences and Engineering, 42, 348.

Gupta, A.K., Velmurugan, R., Joshi, M., Gupta, N.K., 2019, “Studies on shape memory alloy-embedded GFRP composites for improved post-impact damage strength”, INTERNATIONAL JOURNAL OF CRASHWORTHINESS, 24, 363–379.

Ha, S.K., Jin, K.K., Huang, Y., 2008, “Micro-Mechanics of Failure (MMF) for Continuous Fiber Reinforced Composites”, Journal of Composite Materials, 42, 1873-1895.

Herakovich, C.T., 2012, “Mechanics of composites: A historical review”, Mechanics Research Communications, 41, 1–20.

Hinton, M.J., Kaddour, A.S., Soden, P.D., 2004, “Failure Criteria in Fibre-Reinforced-Polymer CompositeS - The World-Wide Failure Exercise”, Elsevier

Hongkarnjanakul, N., Bouvet, C., Rivallant, S., 2013, “Validation of low velocity impact modelling on different stacking sequences of CFRP laminates and influence of fibre failure”, Composite Structures, 106, 549–559.

Kaddour, A.S., Hinton, M.J., 2012, “Input data for test cases used in benchmarking triaxial failure theories of composites”, Journal of Composite Materials, 46, 2295-2312.

Kubair, D.V., Lakshmana, B.K., 2008, “Cohesive modeling of low-velocity impact damage in layered functionally graded beams”, Mechanics Research Communications, 35, 104-114.

Kursun, A., Senel, M., Enginsoy, H.M., Bayraktar, E., 2016, “Effect of impactor shapes on the low velocity impact damage of sandwich composite plate: Experimental study and modelling”, Composites Part B, 86, 143-151.

Lagoudas, D.C., 2008, “Shape memory alloys: modeling and engineering applications”, Springer Science & Business Media.

Lester, B.T., Baxevanis, T., Chemisky, Y., Lagoudas, D.C., 2015, “Review and perspectives: shape memory alloy composite systems”, Acta Mech, 226, 3907–3960.

Lin, C.H., 2022, “Effective properties of 0–3, 1–3, and 2–2 composites based on unified unit-cell micromechanics model”, Mechanics Research Communications, 119, 103807.

Liu, P.F., Liao, B.B., Jia, L.Y., Peng, X.Q., 2016, “Finite element analysis of dynamic progressive failure of carbon fiber composite laminates under low velocity impact”, Composite Structures, 149, 408–422.

Melo, J.D.D., Villena, J.E.N., 2012, “Effect of fiber volume fraction on the energy absorption capacity of composite materials”, Journal of Reinforced Plastics and Composites, 31, 153–161.

Oliveira, L.M., Donadon, M.V., 2020, “Delamination analysis using cohesive zone model: A discussion on traction-separation law and mixed-mode criteria”, Engineering Fracture Mechanics, 228, 106922.

Paiva, A., Savi, M.A., 2006, “An Overview of Constitutive Models for Shape Memory Alloys”, Mathematical Problems in Engineering, 2006, 56876, 1-30.

Pinto, T.H.L., Gul, W., Torres, L.A.G., Cimini Jr., C.A., Ha, S.K., 2021, “Experimental and Numerical Comparison of Impact Behavior between Thermoplastic and Thermoset Composite for Wind Turbine Blades”, Materials, 14, 6377.

Puck, A., Schurmann, H., 1998, “Failure analysis of FRP laminates by means of physically based phenomenological models”, Compos Sci Technol, 58, 1045–67.

Savi, M.A., 2015, “Nonlinear Dynamics and Chaos of Shape Memory Alloy Systems”, International Journal of Non-linear Mechanics, 70, 2-19.

Shah, P.D., Melo, J.D.D., Cimini Jr, C.A., Ridha, M., 2010, “Evaluation of Notched Strength of Composite Laminates for Structural Design”, Journal of Composite Matererials, 44, 2381-2392.

Shahveisi, N., Feli, S., 2022, “Analytical modeling of low-velocity impact LVI on composite pipe with protective GLARE layer and flexible core”, Journal of the Brazilian Society of Mechanical Sciences and Engineering, 44, 92.

Staniszewski, J.M., Boyd, S.E., Bogetti, T.A., 2022, “A multi-scale modeling approach for UHMWPE composite laminates with application to low-velocity impact loading”, International Journal of Impact Engineering, 159, 104031.

Starikov, R., 2013, “Assessment of impact response of fiber metal laminates” International Journal of Impact Engineering, 59, 38-45.

Talreja, R., Phan, N., 2019, “Assessment of damage tolerance approaches for composite aircraft with focus on barely visible impact damage”, Composite Structures, 219, 1–7.

Thiene, M., Galvanetto, U., 2015, “Impact location in composite plates using proper orthogonal decomposition”, Mechanics Research Communications, 64, 1–7.

Tita, V., de Carvalho, J., Vandepitte, D., 2008, “Failure analysis of low velocity impact on thin composite laminates: Experimental and numerical approaches”, Composite Structures, 83, 413–428.

Topac, O.T., Gozluklu, B., Gurses, E., Coker, D., 2017, “Experimental and computational study of the damage process in CFRP composite beams under low-velocity impact”, Composites Part A: Applied Science and Manufacturing, 92, 167-182.

Tsai, S.W., Melo, J.D.D., 2014, “An invariant-based theory of composites”, Composites Science and Technology, 100, 237-243.

Vignoli, L.L., Carneiro Neto, R.R.M., Savi, M.A., Pacheco, P.M.CL., Kalamkarov, A.L., 2021, “Trace theory applied to composite analysis: A comparison with micromechanical models”, Composites Communications, 25, 100715.

Vignoli, L.L., Castro, J.T.P., 2021, “A parametric study of stress concentration issues in unidirectional laminates”, Mechanics of Advanced Materials and Structures, 28, 1554-1569.

Vignoli, L.L., Kenedi, P.P., Mariano, M.J.B., 2022a, “Exploring Thermography Technique to Validate Multiscale Procedure for Notched CFRP Plates”, Composites Part C: Open Access, 7, 100241.

Vignoli, L.L., Savi, M.A. 2018, “Multiscale Failure Analysis of Cylindrical Composite Pressure Vessel: A Parametric Study”, Lat. Am. J. Solids Struct., 15, 1–20.

Vignoli, L.L., Savi, M.A., El-Borgi, S., 2020b, “Nonlinear dynamics of earthquake-resistant structures using shape memory alloy composites”, JOURNAL OF INTELLIGENT MATERIAL SYSTEMS AND STRUCTURES, 31, 771-787.

Vignoli, L.L., Savi, M.A., Pacheco, P.M.CL., Kalamkarov, A.L., 2019, “Comparative analysis of micromechanical models for the elastic composite laminae”, COMPOSITES PART B-ENGINEERING, 174, 106961.

Vignoli, L.L., Savi, M.A., Pacheco, P.M.CL., Kalamkarov, A.L., 2020a, “Multiscale Approach to Predict Strength of Notched Composite Plates”, Composite Structures, 253, 112827.

Vignoli, L.L., Savi, M.A., Pacheco, P.M.CL., Kalamkarov, A.L., 2020c, “Micromechanical analysis of longitudinal and shear strength of composite laminae”, Journal of Composite Materials, 54, 4853-4873.

Vignoli, L.L., Savi, M.A., Pacheco, P.M.CL., Kalamkarov, A.L., 2020d, "Micromechanical analysis of transversal strength of composite laminae", Composite Structures, 250, 112546.
Vignoli, L.L., Savi, M.A., Pacheco, P.M.CL., Kalamkarov, A.L., 2022b, "A Novel Micromechanical Model for Elastic Properties of Unidirectional Composites with Circular Fibers", Applied Composite Materials, in press.
Wang, A., Wang, X., Xian, G., 2021, "The influence of stacking sequence on the low-velocity impact response and damping behavior of carbon and flax fabric reinforced hybrid composites", Polymer Testing, 104, 107384.
Wang, F., Wang, B., Kong, F., Ouyang, J., Ma, T., Chen, Y., 2021, "Assessment of degraded stiffness matrices for composite laminates under low-velocity impact based on modified characteristic length model", Composite Structures, 272, 114145.
Zhao, S., Teng, J., Wang, Z., Sun, X., Yang, B., 2018, "Investigation on the Mechanical Properties of SMA/GF/Epoxy Hybrid Composite Laminates: Flexural, Impact, and Interfacial Shear Performance", Materials, 11, 246.

7. RESPONSIBILITY NOTICE

The authors are the only responsible for the printed material included in this paper.